Accepted Manuscript

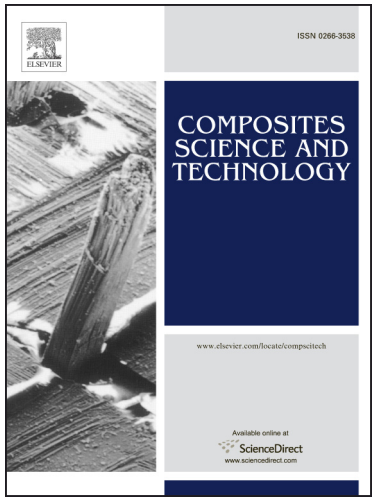

Temperature dependence of the interfacial shear strength in glass-fibre epoxy composites

J.L. Thomason, L. Yang

PII: S0266-3538(14)00084-0
DOI: http://dx.doi.org/10.1016/j.compscitech.2014.03.009
Reference: CSTE 5764

To appear in: *Composites Science and Technology*

Received Date: 18 December 2013
Revised Date: 6 March 2014
Accepted Date: 8 March 2014

Please cite this article as: Thomason, J.L., Yang, L., Temperature dependence of the interfacial shear strength in glass-fibre epoxy composites, *Composites Science and Technology* (2014), doi: http://dx.doi.org/10.1016/j.compscitech.2014.03.009

This is a PDF file of an unedited manuscript that has been accepted for publication. As a service to our customers we are providing this early version of the manuscript. The manuscript will undergo copyediting, typesetting, and review of the resulting proof before it is published in its final form. Please note that during the production process errors may be discovered which could affect the content, and all legal disclaimers that apply to the journal pertain.

ACCEPTED MANUSCRIPT

Temperature dependence of the interfacial shear strength in glass-fibre epoxy composites.

J. L. Thomason* and L. Yang

University of Strathclyde, Department of Mechanical and Aerospace Engineering, 75 Montrose Street, Glasgow G1 1XJ, United Kingdom.

*Corresponding Author, james.thomason@strath.ac.uk Tel:0044-141-5482691

Abstract

The present work focuses on further investigation of the hypothesis that a significant fraction of apparent interfacial shear strength (IFSS) in fibre-reinforced composites can be attributed to a combination of residual radial compressive stress and static friction at the fibre-polymer interface. The temperature dependence of the interfacial properties of a glass fibre-epoxy system has been quantified using the laboratory developed TMA-microbond technique. The temperature dependence of apparent IFSS of glass fibre - epoxy in the range 20°C up to 150°C showed a significant inverse dependence on testing temperature with a major step change in the glass transition region of the epoxy matrix. It is shown that the magnitude of the residual radial compressive stress at the interface due to thermal and cure shrinkage is of the same order of magnitude as the measured IFSS. It is concluded that it possible to suggest that residual stress combined with static adhesion could be the major contributor to the apparent interfacial adhesion in glass fibre – epoxy systems.

Keywords: A Glass fibres, B Fibre/matrix bond, B Interfacial strength, C Residual stress

ACCEPTED MANUSCRIPT

1. Introduction

There has been a rapid growth in the development and application of fibre-reinforced polymer composites in recent years. Parallel to this growth has been the increasing recognition of the need to better understand and measure the micro-mechanical parameters that control the structure–property relationships in such composites. Composite properties result from a combination of the fibre and matrix properties and the ability to transfer stresses across the fibre–matrix interface. Optimization of the stress transfer capability of the fibre-matrix interface region is critical to achieving the required composite performance level. The ability to transfer stress across this interface is often reduced to a discussion of 'adhesion' that is a simple term to describe a combination of complex phenomena on which there is still significant debate as to their relative significance and their characterisation. Certainly, one of the generally accepted manifestations of 'adhesion' is the mechanically measured value of interfacial shear strength (IFSS). Despite the high level of attention commonly focussed on chemical influences, such as the application of silane and polymeric coupling agents, on the level of composite IFSS. A number of authors have also commented on the role of shrinkage stresses contributing to the stress transfer capability at the fibre-matrix interface [1-10]. Most composite materials are processed at elevated temperature and then cooled. Since in most cases, the thermal expansion coefficients of matrix polymers are much greater than that of the reinforcement fibres, this cooling process results in a build-up of compressive radial stress (σ_R) at the interface. Assuming that the coefficient of static friction (μ_s) at the interface is non-zero these compressive stresses will contribute a frictional component $\tau_{fs} = \mu_s.\sigma_R$ to the apparent shear strength of the interface. In the case of thermoplastic polymer matrices where there may often be little or no chemical bonding across the interface, these static frictional stresses can make up a large fraction

ACCEPTED MANUSCRIPT

of the apparent IFSS [9,10]. Most of the available models [1-6] of this phenomenon indicate that the level of residual compressive stress at the interface should be directly proportional to ΔT, the difference between matrix solidification temperature and the composite operating or test temperature. Consequently, this implies that the apparent IFSS in composites should also be dependent on the test temperature.

We recently reported the development of the TMA-microbond apparatus that allows for the measurement of IFSS using the microbond test operated in the temperature controlled environment of a thermo-mechanical analyser [9,11]. Using this equipment to measure the apparent IFSS in a glass fibre – polypropylene (GF-PP) system it was found that the IFSS showed a highly significant inverse dependence on testing temperature with a major increase in the glass transition region of the PP matrix [9]. Further analysis showed that approximately 70% of the apparent room temperature IFSS in this system can be attributed to residual radial compressive stress at the fibre-matrix interface. These results are in good agreement with those of Wenbo *et al* who recently reported the use of similar methods to show that 80% of the apparent IFSS in a carbon fibre reinforced poly(phthalazinone ether ketone) system could be attributed to residual radial compressive stress at the interface [10]. Whereas this concept is readily understandable in thermoplastic systems where there may be little or no expectation of chemical bonding across the interface, it becomes challenging to expectations in thermosetting matrix systems where there is a long history of the use of chemical bonding theory at the interface. The microbond test was originally developed [12] to deal with the challenge of characterizing the fibre-matrix interface in systems with high levels of apparent adhesion such as those often experienced with epoxy resin matrices. Despite the long history of the application of the microbond test in this area there

ACCEPTED MANUSCRIPT

appears to have been little, if any, investigation of temperature effects such as those suggested above. Nevertheless, a number of authors [3-5] have reported temperature dependence of the apparent IFSS in epoxy-based systems obtained using the fragmentation test. However, this has not been investigated systematically and there has been little work recently reported on this important subject. In order to explore these concepts further we have investigated the application of the TMA-microbond technique to the characterisation of the IFSS in a glass fibre – epoxy (GF-EP) system. In this paper we present and discuss results on the apparent IFSS of the GF-EP system over the temperature range 20°C-150°C.

2. Materials and Methods

2.1 Materials

Boron free E-glass fibres (average diameter = 17.5μm) coated with γ-aminopropyltrimethoxysilane were supplied by Owens Corning-Vetrotex [13]. IFSS was measured using the in-laboratory developed TMA-microbond test technique. The reproducible preparation of microbond samples is critical to the outcome of the measurement and the avoidance of erroneous interpretation of test results [9,11]. Individual fibres were carefully selected from the roving bundles and 80 mm lengths were mounted on wire frames. The epoxy resin and curing agent used were Araldite 506 (Sigma-Aldrich) and Triethylenetetramine (TETA) hardener (Sigma-Aldrich). The resin and hardener were thoroughly mixed in stoichiometric proportions (22:3) recommended by the manufacturer and degassed under vacuum for 12 minutes. Epoxy droplets were then deposited on a single fiber using a thin wire that had a small resin bead on its tip.

ACCEPTED MANUSCRIPT

Approximately 40 droplets were placed on individual fibres before these samples were transferred into a convection oven, where they were heated first to 60°C and held isothermally for 1 hour followed by another 2 hours heating at 120°C. After heating, the samples were left in the oven to cool down. The state of cure of the epoxy resin system was examined using differential scanning calorimetry (DSC) in a TA Instruments Q2000 DSC with a heating/cooling rate of 10°C/min and a 5-6 mg sample size. Results indicated that there was no further exothermic event detectable in a temperature range from 20°C up to 200°C for the cured epoxy and that the polymer glass transition temperature (Tg) occurred in the range 60°C<Tg<80°C. Prior to testing the microbond samples were examined using a Nikon Epiphot inverted microscope (x200 magnification) in order to determine the fibre diameter (D_f), embedded fibre length (L_e), and the maximum droplet diameter (D_m).

2.2 TMA-Microbond

Development of the TMA-Microbond test (TMA-MBT) has abeen reported previously [9,11]. Figure 1 shows the experimental setup for the TMA-MBT. The droplet sits on a shearing plate, which rests on a stationary quartz probe. The movable probe, concentrically installed with the stationary probe, rests on the paper tab attached to the glass fibre as shown in Figure 1. This assembly is enclosed in the TMA temperature controlled programmable oven. Interfacial shear stress can be generated at the desired isothermal temperature by pulling down the paper tab using the movable probe. The free fibre length between the tab and the polymer droplet was set at a constant value of 5 mm and the rate of fibre displacement was 0.1 mm/min. The load-displacement curve from each test was recorded to obtain the maximum force (F_{max}) at debonding. This was

ACCEPTED MANUSCRIPT

used with the corresponding fibre diameter and embedded length to calculate the apparent IFSS using to Equation 1.

$$\tau_{ult} = \frac{F_{max}}{\pi D L_e} \quad (1)$$

In order to fully understand and interpret the temperature dependence of the IFSS measured using the TMA-MBT test it was also necessary to carry out a full thermo-mechanical characterisation of the properties the cured epoxy matrices and single glass fibres using dynamical mechanical analysis, differential scanning calorimetry and thermo-mechanical analysis. Dynamic mechanical analysis (DMA) was carried out on cured samples of the epoxy system with dimensions 60x12.6x3.2 mm using a TA Instruments Q800 DMA. Three-point bending configuration was used with a support span length of 50 mm and a heating rate 3°C/min from 20°C to 200°C, frequency 1 Hz, oscillating amplitude 100 µm, static pre-load 0.1 N, and force track: 150%. The coefficient of linear thermal expansion (CLTE) of discs with dimensions of 6x1.6 mm was measured using a Q400EM TMA with heating rate 3°C/min from 20°C to 200°C with a 0.1 N static force. Axial CLTE of 20 mm lengths of single unsized glass fibre was also determined using a Q400EM TMA heated at 3°C/min from -60°C to 500°C under 50ml/min nitrogen [14].

3. Results

The TMA-microbond results for F_{max} versus interfacial area obtained for the glass fibre – epoxy (GF-EP) system at seven different test temperatures in the range 20°C to 150°C are shown in Figure 2. It can be seen that nearly all data sets exhibit a strong linear relationship with a low level of scatter, high values of R^2. In particular, the data sets obtained well above or below the matrix glass transition temperature (Tg) show low

ACCEPTED MANUSCRIPT

levels of scatter with high levels of slope below Tg and low levels of slope above Tg. However, the data set obtained at 80°C shows a very much higher level of scatter. Clearly there is a large change in the magnitude of the IFSS around the matrix Tg and consequently it is not surprising that the data obtained at 80°C show large levels of scatter. Further examination of Figure 2 reveals that for data sets obtained above Tg the extrapolated lines pass through (or close to) the origin as predicted from Equation 1. However, the data sets obtained below Tg all show extrapolated lines that clearly do not pass through the origin. We have previously observed that, if a microbond data set does not extrapolate through the origin, this is a strong indication of some unexpected experimental parameter that is unaccounted for [15,16]. In the case of GF-PP, SEM examination of post-debond samples led us to understand that the need to avoid thermal-oxidative degradation of the PP during sample preparation was critical to obtaining reproducible results from the microbond test. For this reason we also undertook a series of SEM analyses of post-debond GF-EP samples tested at different temperatures.

The key result from this SEM analysis is illustrated in Figure 3. It was found that all GF-EP samples tested above Tg (Figure 3b) revealed a fully debonded, relatively undamaged, epoxy droplet still remaining on the fibre. However, virtually all samples debonded below Tg were found to be very similar in appearance to the sample shown in Figure 3a. It can be seen that a substantial fraction of the droplet which was close to the knife edges has not been debonded at the fibre-matrix interface. Instead it appears that the fracture has propagated into the matrix from the knife edges until reaching the fibre and then the crack has proceeded further along the fibre-matrix interface. Consequently, it was necessary to correct the values of the embedded length used in Equation 1 (or the

ACCEPTED MANUSCRIPT

interfacial area used in Figure 5) to account for the reduction in the actual debonded interfacial area in these samples. Figure 4 shows the TMA-microbond results for F_{max} versus corrected embedded area obtained for the GF-EP system at the seven different test temperatures. It can be seen that all extrapolated lines now pass through (or close to) the origin as predicted in Equation 1.

The results for average IFSS obtained for GF-EP at test temperatures are summarized in Figure 5 that shows the average values with 95% confidence limits (between 10-20 individual measurements per temperature). For comparison we also show IFSS data previously obtained for a GF-PP system using the same TMA-microbond technique. It can be clearly seen that there exists a significant temperature dependence of measured IFSS in this thermosetting system. The IFSS drops from 54 MPa at 20°C to just 2 MPa at 150°C. It is noticeable that the highest rate of change of IFSS with temperature is also in the region of the glass transition temperature of the epoxy matrix with 1.1MPa/°C at 70°C. This value is almost five times higher than that in GF-PP at 20°C and this clearly plays a role in the high degree of scatter observed in Figure 4 for the data obtained at 80°C. The magnitude for the IFSS of GF-EP is clearly much greater than for GF-PP at any particular temperature. This supports the general expectation that the stress transfer capability of the GF-EP interface is much greater than that of GF-PP. However, there is also a striking similarity in the form of the IFSS versus temperature dependence for these two very different composite systems. Both systems exhibit a significant step-change in the IFSS around the associated matrix Tg.

4. Discussion

ACCEPTED MANUSCRIPT

ACCEPTED MANUSCRIPT

Those familiar with DMA of polymers will recognise the similarity between the IFSS data in Figure 5 and the typical DMA results for the storage modulus of many polymers across temperature range that includes the polymer Tg. This similarity is clearly visible in Figure 6 which shows the results for the IFSS results from Figure 5 normalised to the highest value obtained for each system compared to the normalised DMA storage modulus data obtained for the matrix system. The similarity in the shape of the data curves is striking. Indeed it is possible to further explain some of the apparent shift in temperature between the IFSS and modulus data as being due to the IFSS measurements being made isothermally in one instrument and the modulus data being obtained from a dynamic heating scan in a different instrument. Consequently the overlap of the two types of measurement may be even closer than presented in Figure 6. This correlation is further examined in Figure 7 where the normalised IFSS data is plotted directly against the appropriate normalised matrix modulus. With the exception of the IFSS value for GF-EP at 80 °C, which has a very large degree of scatter, the data from these two very different matrix systems appear to fall on the same straight line relationship. This result of a strength based IFSS value apparently correlating so well with the matrix modulus, obtained at low strain, is intriguing and begs further explanation. Similar correlation between IFSS measured by fragmentation test and matrix modulus has been reported for carbon fibre-epoxy [4,5] and related to the change in matrix and interphase shear properties.

As previously discussed, an increase in IFSS with decreasing temperature is a phenomenon which would be expected if compressive residual stresses and interfacial static friction play a significant role in the interfacial stress transfer capability in this

ACCEPTED MANUSCRIPT

system. If the temperature dependence of the fibre and matrix modulus and expansion coefficients is known then the residual compressive stress (σ_R) at the fibre-matrix interface can be calculated from available models [1-6]. Raghava proposed that the radial stresses due to thermal shrinkage can be calculated from

$$\sigma_R = \frac{(\alpha_m - \alpha_f)(T_s - T_t)E_f E_m}{(1+\nu_f+2V_f)E_f + (1+\nu_m)E_m} \quad (2)$$

where α is the thermal expansion coefficient, T_s is the stress free temperature where matrix solidification begins, T_t is the testing temperature, ν is the Poisson ratio, V_f is the fibre volume fraction, E is the modulus and f and m are subscripts for the fibre and matrix respectively [2]. For many composite systems Ef>>Em, in which case equation 2 approximates that σ_R scales with the magnitude of $\Delta\alpha\Delta T.E_m$. This could already be a good explanation of the general form of the temperature dependence of IFSS in Figure 5 appearing remarkably similar to the temperature dependence of E_m seen in Figures 6.

Nairn developed a more complex model [1] that accounted for the effects of differences in the axial and transverse fibre properties, and Wagner and Nairn later expanded that model to allow for the presence of an intermediate interphase in the system [6]. The reader is referred to the original manuscripts for the details of these models, however they basically require similar input parameters to equation 2 and the results for residual stress are of similar magnitude when isotropic fibres such as glass are being considered. These models also predict a volume fraction dependence of the residual stress, however it was found that this only began to show any significant effects when V_f exceeded 10%. The average V_f for the microbond samples used to generate the data in Figure 4 was found to be 1.2%.

ACCEPTED MANUSCRIPT

Figure 8 shows the results for the thermo-mechanical characterisation of the epoxy matrix obtained by TMA and DMA. The data shows that the both the modulus and expansion coefficient of the epoxy matrix are strongly dependent on the temperature and this must be incorporated into the calculations. Glass fibre properties are also temperature dependent but on a much less significant scale and can be considered constant in this temperature range, a value of $\alpha_f = 6.0 \times 10^{-6}$ m/m was measured for the fibres used in this study [14]. The build-up of residual compressive radial stress at the GF-epoxy interface was calculated in steps of 10°C using equation 2 and the above input data. As previously discussed, if the magnitude of the coefficient of static friction for glass-epoxy is known then contribution of σ_R to the apparent IFSS can be calculated. There is very little information available on μ_s in the literature, however Schoolenberg reported an experimental value for $\mu_s = 0.65$ in a sized glass fibre-polypropylene system [17]. Detassis used a value of $\mu_s = 0.6$ for a carbon fibre – epoxy system [5].

In combination with an interfacial radial residual thermal stress calculated using equation 2 this value was shown to predict well the magnitude and temperature dependence of the IFSS in the GF-PP system [9]. The results obtained using equation 2 for the residual interfacial radial stress in the current GF-EP system are shown in Figure 9. It can be seen that, in order to be able to generate a reasonable approximation to the IFSS results for GF-EP a very high level of μ_s (>6) would be required. A similar low level of contribution of thermal stresses to the interfacial stress transfer capability in carbon fibre – epoxy has been reported [4,5]. Proponents of the hypothesis that chemical bonding should be considered as the main principal mechanism accounting for the measured high level of IFSS in GF-EP may not be surprised by this result. Nevertheless, it is still fascinating to observe that the IFSS obtained from these two

ACCEPTED MANUSCRIPT

systems both exhibit a strong correlation with the temperature dependence of the matrix modulus.

One significant difference in the residual stress and strain in the thermosetting (epoxy) and thermoplastic (polypropylene) systems is the fact that thermosetting systems also have a level of shrinkage related to volume changes during polymerisation known as cure shrinkage. Cure shrinkage can result in significant volume changes of epoxy resins undergoing isothermal curing with values up to -7% being observed [18-20]. In a recent paper Jakobsen actually suggested that the residual stresses in an Eglass-epoxy composite were mainly due to the result of cure shrinkage rather than the mismatch between the fibre and matrix thermal expansion coefficients [18]. An important question here would be how much of the cure shrinkage occurs before the gel point of the epoxy system. It can be assumed that in the early stages of the epoxy polymerization any cure shrinkage can relax away due to the low molecular weight liquid nature of the matrix. Gelation is the liquid-solid transition of the epoxy resin that occurs when the average molecular weight approached infinity. One can reasonably assume that strain induced by cure shrinkage will require more time to relax away as the system approaches the gel point and presumably once the gel point is exceeded then further cure shrinkage related residual strain will be locked into the epoxy network. As the system is cooled through Tg the matrix modulus increases and consequently the residual stress from this locked in cure shrinkage strain will increase in proportion to the matrix modulus. This hypothesis would appear to fit quite well with the observed IFSS dependence of temperature observed in Figure 4. In Figure 9 we show the additional residual stress that would be present in our system assuming an isothermal volumetric cure shrinkage value of -6%. It can be seen that the residual radial interfacial stress obtained from such a

ACCEPTED MANUSCRIPT

level of cure shrinkage is significantly greater than the residual thermal stress. This result appears to be well aligned with the statement of Jakobsen discussed above [18].

It is clear from the data in Figure 9 that the sum of thermal and cure shrinkage related residual radial interfacial stress is of an appropriate magnitude in order for more realistic values of μ_s (<1) to deliver an interfacial stress transfer contribution of the same order of magnitude as the experimentally determined IFSS. We have previously presented data that indicated that a large fraction of the IFSS in a glass fibre - polypropylene system could be attributed to residual radial compressive stresses at the interface [9]. It appears from the current results that it is also possible to make the case for residual stress combined with static adhesion being the major contributor to the apparent interfacial adhesion in a glass fibre – epoxy system.

5. Conclusions

The temperature dependence of the interfacial properties of a glass fibre-epoxy system has been quantified using the laboratory developed TMA-microbond technique. The temperature dependence of apparent interfacial shear strength of glass fibre - epoxy in the range 20°C up to 150°C showed a highly significant inverse dependence on testing temperature with a major step change in the glass transition region of the epoxy matrix. This temperature dependence of the glass fibre - epoxy IFSS was compared to the change in residual radial compressive stresses at the interface as the test temperature is changed. The analysis indicated that the magnitude of the thermal residual stress due to mismatch in the thermal expansion coefficients of fibre and matrix was insufficient to explain the magnitude the of system IFSS. However, when the additional potential

ACCEPTED MANUSCRIPT

residual stress generated by the isothermal cure shrinkage of the epoxy matrix was considered, then the magnitude of the residual stress at the interface could be found to be of the same order of magnitude as the measured IFSS. In a previous similar paper studying temperature dependence of the IFSS in a glass fibre – polypropylene system we concluded that that a large fraction of the IFSS could be attributed to residual radial compressive stresses at the interface. It was concluded from the data presented here that it also possible to suggest that residual stress combined with static adhesion could be the major contributor to the apparent interfacial adhesion in glass fibre – epoxy systems.

References

1. Nairn JA. Thermoelastic analysis of residual stresses in unidirectional, high-performance composites. Polym Compos 1985;6:123-30.

2. Raghava RS, Thermal expansion of organic and inorganic composites. Polym Compos 1988;9:1-11.

3. Di Landro L, Pegoraro M., Evaluation of residual stresses and adhesion in polymer composites. Compos Part A 1996;27:847-53.

4. A. Pegoretti, C. Della Volpe, M. Detassis, C. Migliaresi, H.Wagner, Thermomechanical behaviour of interfacial region in carbon fibre/epoxy composites. Compos Part A 1996;27:1067-1074.

5. M. Detassis, A. Pegoretti, C. Migliaresi, Effect of temperature and strain rate on interfacial shear stress transmission in carbon/epoxy model composites. Compos Sci Technol 1995;53:39-46.

6. Wagner HD, Nairn JA. Residual thermal stresses in three concentric transversely isotropic cylinders. Compos Sci Technol 1997;57:1289-1302.

ACCEPTED MANUSCRIPT

ACCEPTED MANUSCRIPT

7. Thomason JL. Interfacial strength in thermoplastic composites – at last an industry friendly measurement method? Compos Part A 2002;33:1283-8.

8. Thomason JL, Dependence of interfacial strength on the anisotropic fiber properties of jute reinforced composites. Polym Compos 2010;31:1525–34.

9. Thomason JL, Yang L. Temperature dependence of the interfacial shear strength in glass-fibre polypropylene composites. Compos Sci Technol 2011;71:1600-1605.

10. WenBo L, Shu Z, LiFeng H, WeiCheng J, Fan Y, XiaoFei L, RongGuo W. Interfacial shear strength in carbon fiber-reinforced poly(phthalazinone ether ketone) composites. Polym Compos, 2013;34:1921-1926.

11. Yang L, Thomason JL. Development and Application of Micromechanical Techniques for Characterising Interface Strength in Fibre-Thermoplastic Composites. Polymer Testing 2012;31:895–903.

12. Miller B, Muri P, Rebenfeld L. A microbond method for determination of the shear-strength of a fiber-resin interface. Compos Sci Technol 1987;28:17-32.

13. Yang L, Thomason JL. Effect of Silane Coupling Agent on Mechanical Performance of Glass Fibre. J Mater Sci 2013;48:1947-1954.

14. Yang L, Thomason JL. The thermal behaviour of glass fibre investigated by thermomechanical analysis. J Mater Sci 2013;48:5768-5775.

15. Yang L, Thomason JL. Interface strength in glass fibre-polypropylene measured using the fibre pull-out and microbond methods. Compos Part A 2010;41:1077-83.

16. Yang L, Thomason JL, Zhu W Z. The Influence of Thermo-oxidative Degradation on the Interface Strength of Glass-Polypropylene. Compos Part A 2011;42;1293–1300.

17. Schoolenberg GE. In: Karger-Kocsis J. editor. Polypropylene: Structure, Blends and Composites, Chapter 3.6. Chapmann and Hall; 1995.

ACCEPTED MANUSCRIPT

ACCEPTED MANUSCRIPT

18. Jakobsen J, Jensen M, Andreasen JH. Thermo-mechanical characterisation of in-plane properties for CSM E-glass epoxy polymer composite materials – Part 1: Thermal and chemical strain, Polymer Testing 2013;32:1350-1357

19. Li C, Potter K, Wisnom MR, Stringer G. In-situ measurement of chemical shrinkage of MY750 epoxy resin by a novel gravimetric method. Compos Sci Technol 2004;64:55-64.

20. Hoa SV, Ouellette P, Ngo TD. Determination of Shrinkage and Modulus Development of Thermosetting Resins. J Compos Materials 2009;43:783-803.

ACCEPTED MANUSCRIPT

ACCEPTED MANUSCRIPT

Figure Captions

Figure 1. Schematic and close up photograph of the TMA-Microbond test configuration

Figure 2. TMA-microbond peak load versus embedded area for GF-EP at various test temperatures (▲20°C, O 40°C, ◆ 60°C, □ 80°C, ● 100°C, ◇120°C, ■ 150°C).

Figure 3. SEM examination of debonded microdroplets.

Figure 4. TMA-microbond peak load versus corrected debonded area for GF-EP (▲20°C, O 40°C, ◆ 60°C, □ 80°C, ● 100°C, ◇120°C, ■ 150°C).

Figure 5. Comparison of average IFSS versus test temperature temperatures (● GF-EP, ▲ GF-PP)

Figure 6. ▲Epoxy matrix storage modulus and ● coefficient of linear thermal expansion versus temperature

Figure 7. Comparison of normalised IFSS and normalised matrix storage modulus.

Figure 8. Normalised IFSS versus normalised matrix storage modulus.

Figure 9. Comparison of GF-EP IFSS with calculated residual radial interfacial stresses.

ACCEPTED MANUSCRIPT

ACCEPTED MANUSCRIPT

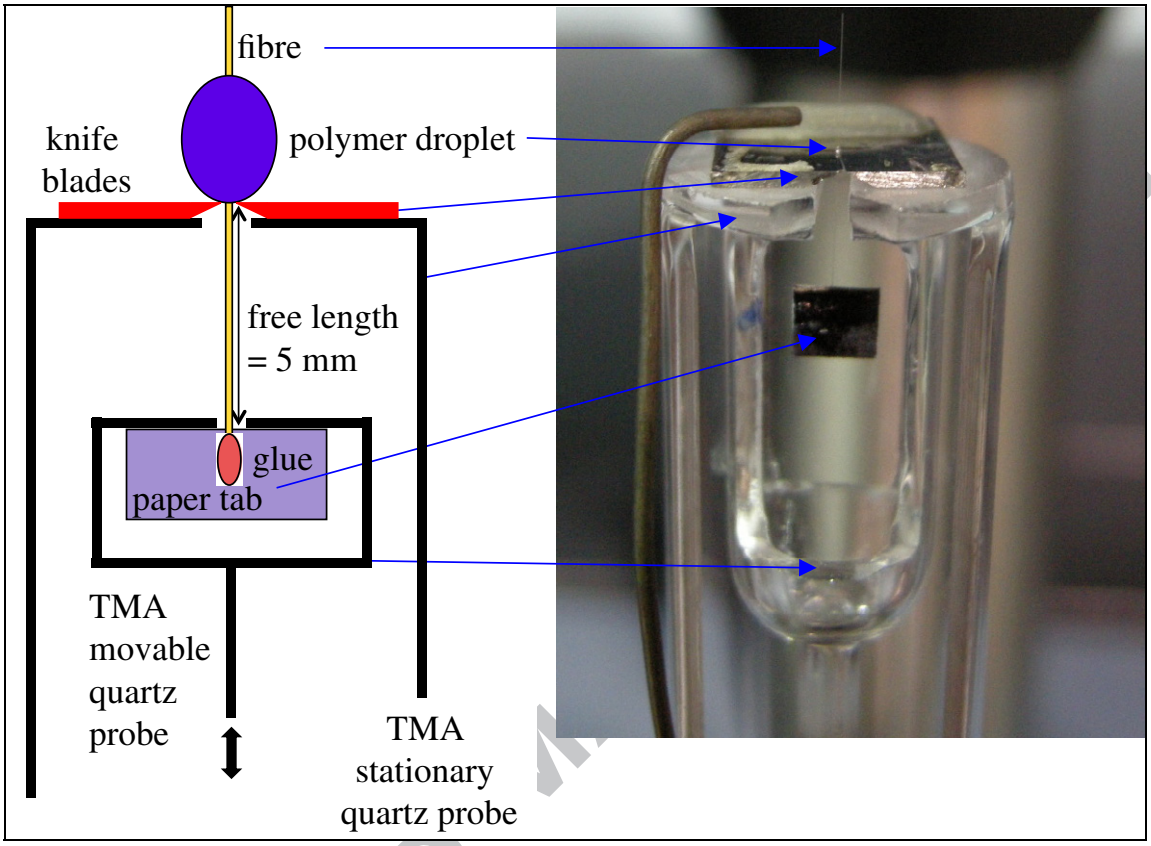

Figure 1. Schematic and close up photograph of the TMA-Microbond test configuration

ACCEPTED MANUSCRIPT

ACCEPTED MANUSCRIPT

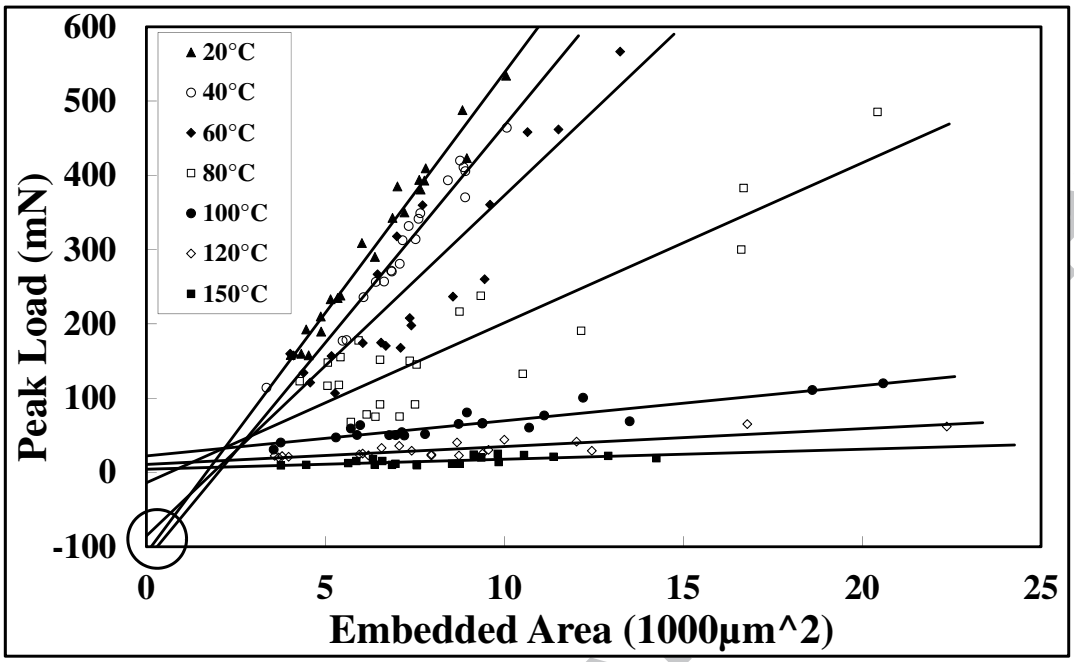

Figure 2. TMA-microbond peak load versus embedded area for GF-EP at various test temperatures (▲20°C, O 40°C, ◆ 60°C, □ 80°C, ● 100°C, ◇120°C, ■ 150°C).

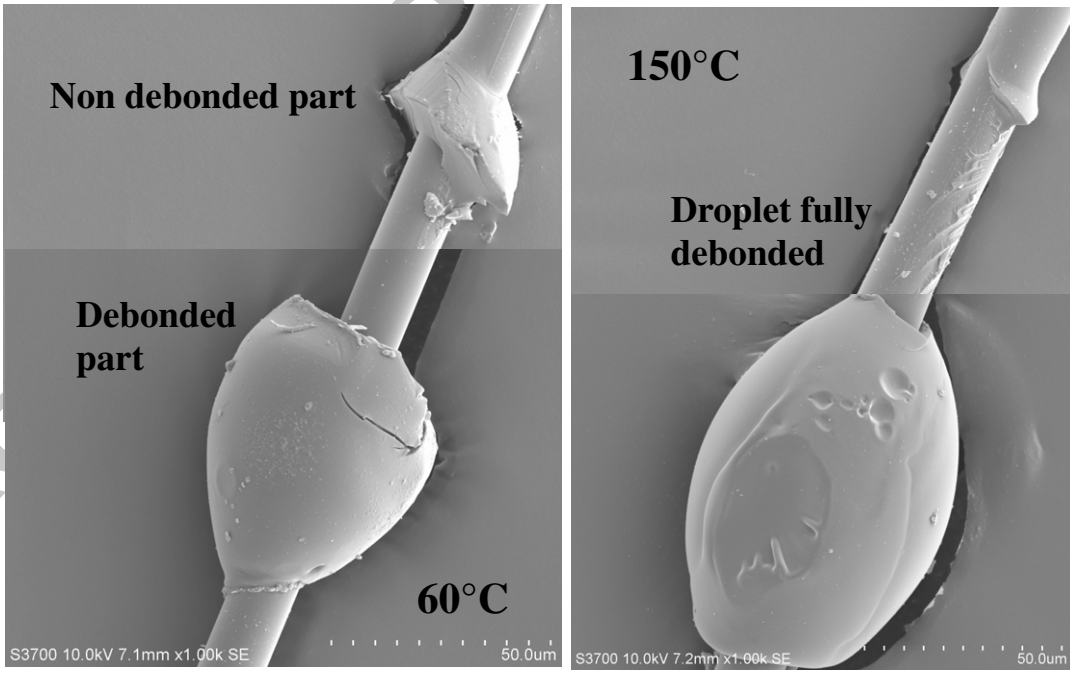

Figure 3. SEM examination of debonded microdroplets

ACCEPTED MANUSCRIPT

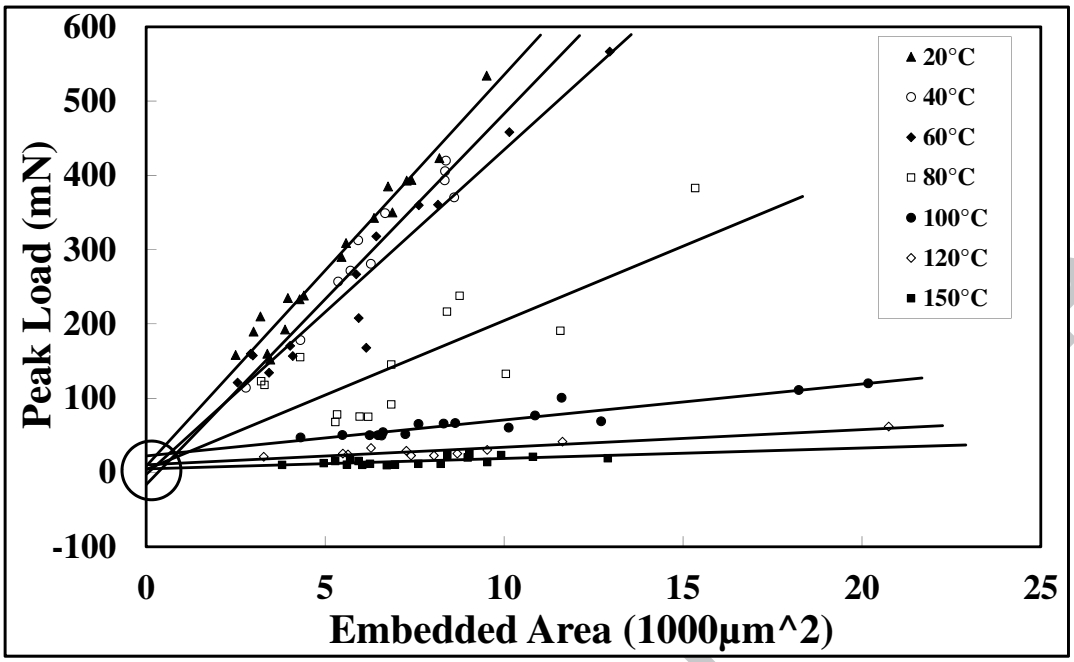

Figure 4. TMA-microbond peak load versus corrected debonded area for GF-EP (▲20°C, O 40°C, ◆ 60°C, □ 80°C, ● 100°C, ◇120°C, ■ 150°C).

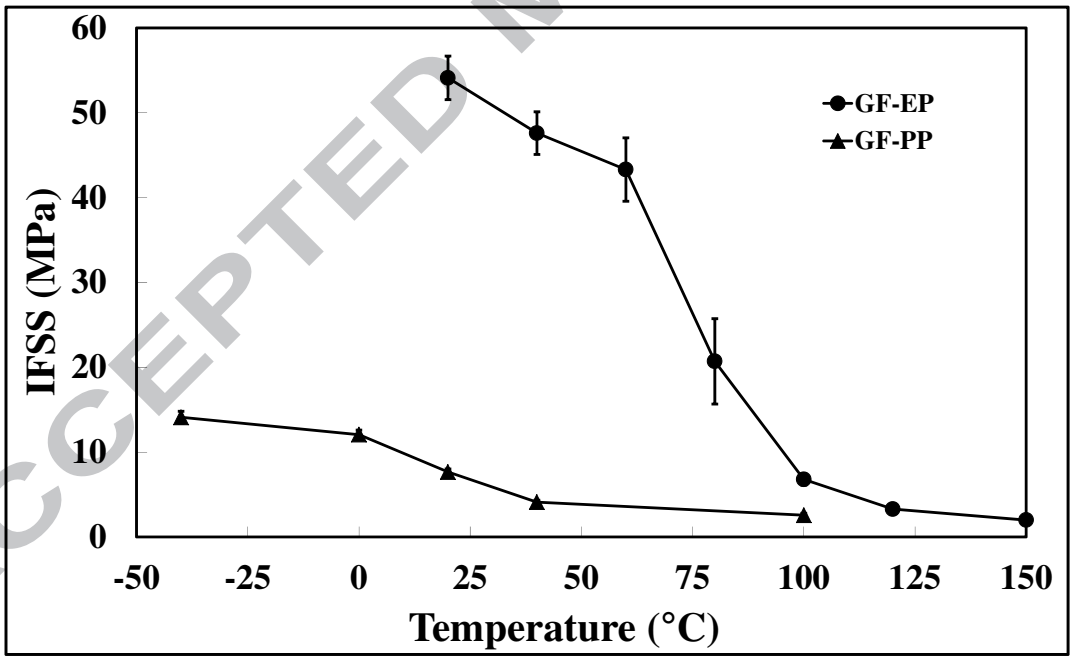

Figure 5. Comparison of average IFSS versus test temperature temperatures (● GF-EP, ▲ GF-PP)

ACCEPTED MANUSCRIPT

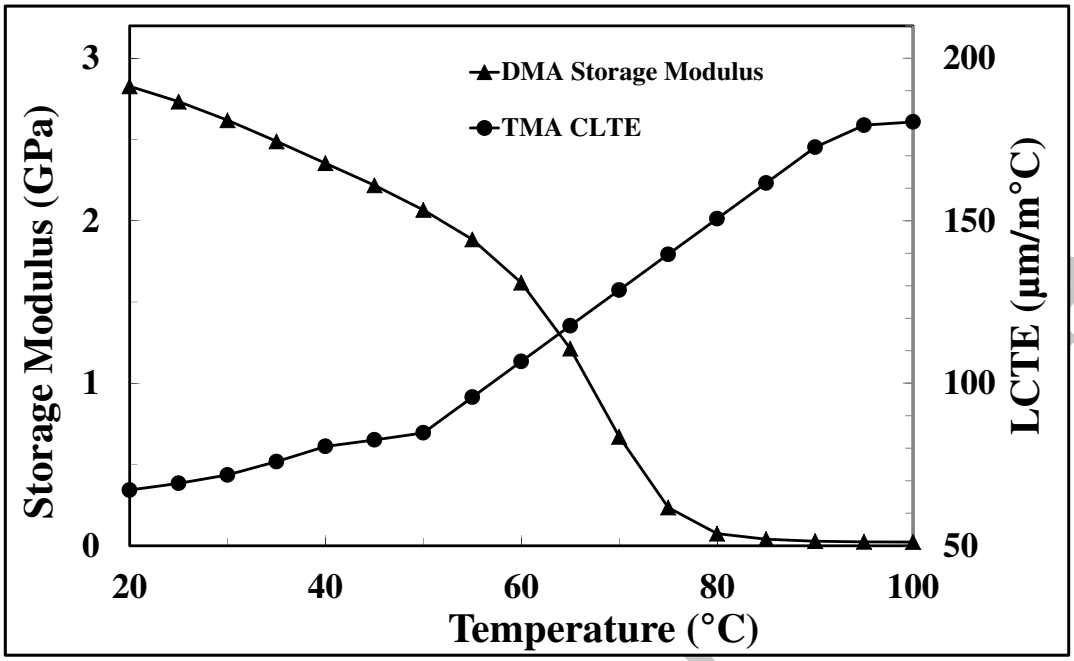

Figure 6. ▲ Epoxy matrix storage modulus and ● coefficient of linear thermal expansion versus temperature.

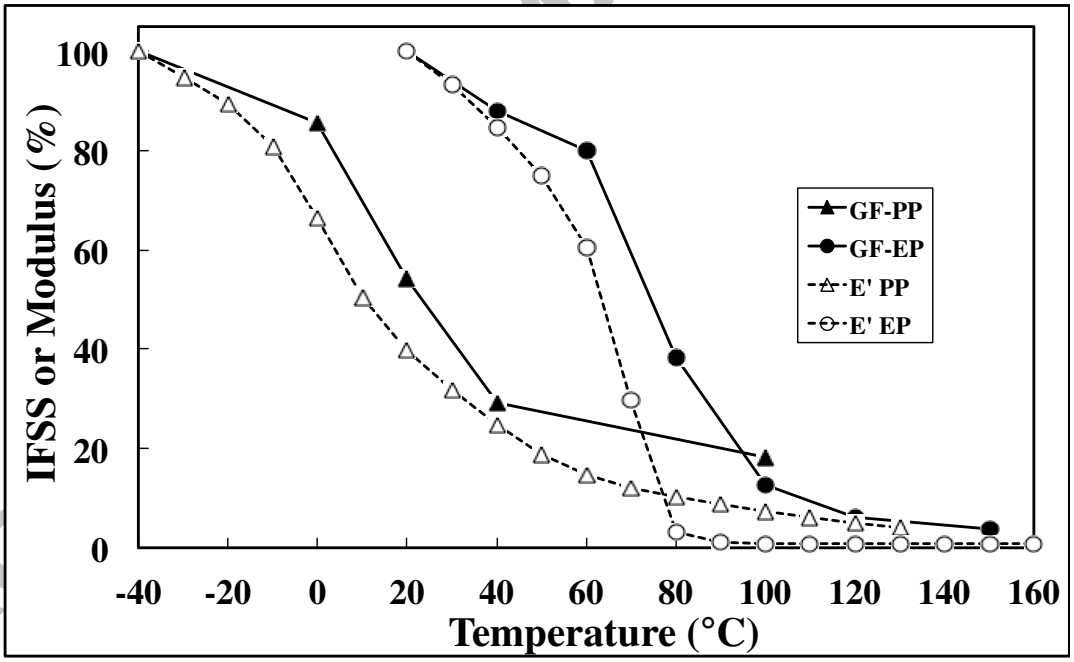

Figure 7. Comparison of normalised IFSS and normalised matrix storage modulus.

ACCEPTED MANUSCRIPT

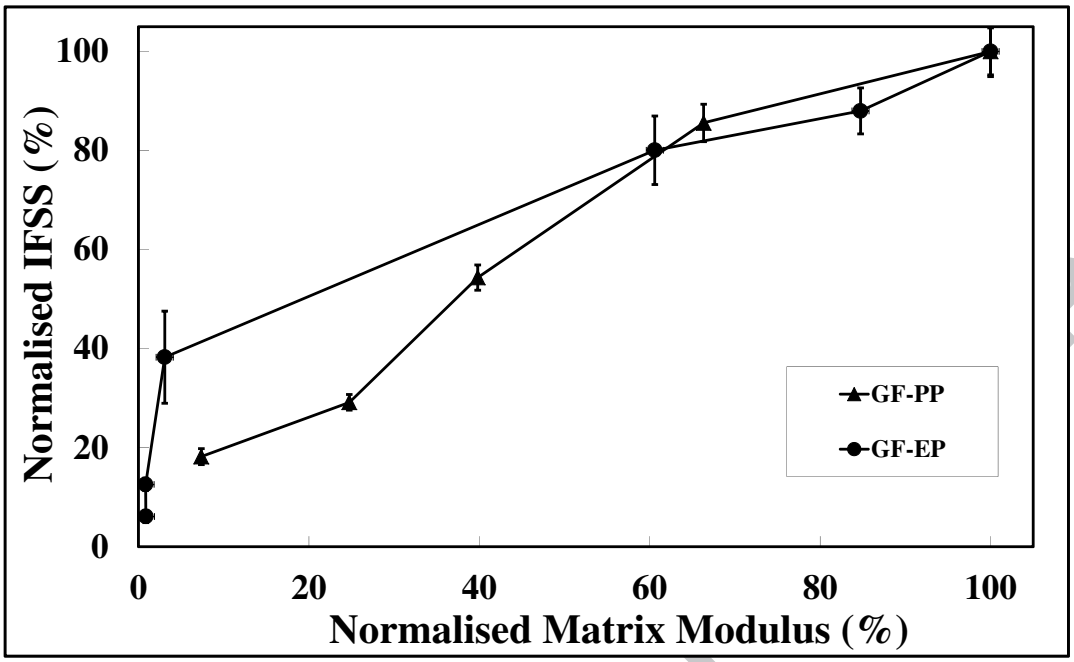

Figure 8. Normalised IFSS versus normalised matrix storage modulus.

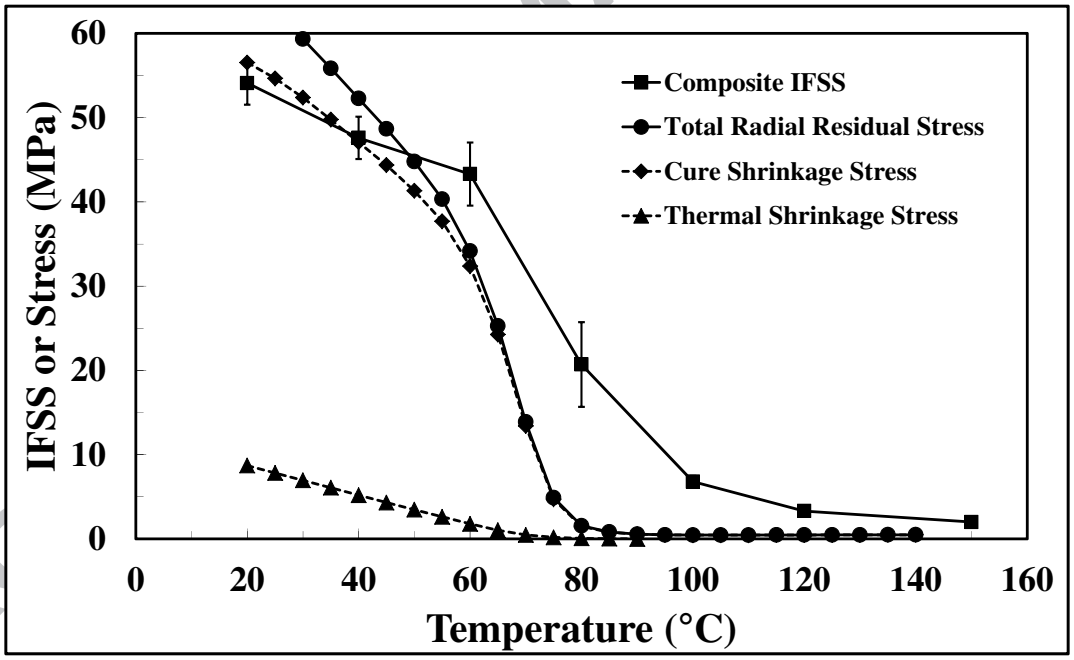

Figure 9. Comparison of GF-EP IFSS with calculated residual radial interfacial stresses.